14 Reconfigurable Wearable Antennas

Sema Dumanli

CONTENTS

14.1 INTRODUCTION

Various wearable sensors are being introduced to the market; they monitor diverse physiological parameters for fitness tracking of healthy individuals or the diagnosis, therapy, and rehabilitation of patients [1–3]. In the future, it is envisaged that each person is going to be wearing multiple sensors on their body that are part of a body area network (BAN). Some common challenges for wearable sensors can be listed as: achieving robust and quality sensing, high-level integration hence low-cost production, longer battery lifetime, and user convenience [4]. Although wearable sensor design is highly multidisciplinary, it can be argued that the careful design of the wireless links is essential to the solution of the previously mentioned goals. These links within the BANs are classified under three categories: in-body, on-body, and off-body [5]. The links that a wearable sensor forms with an implantable device are called in-body links. On-body links are the links created between two wearable devices and, finally, the links that a wearable sensor form with an off-body device, such as an access point, are called off-body links.

This chapter discusses antenna solutions for wearable devices; therefore, all of these propagation links are going to be taken into consideration. The network architecture

should be designed so that the challenges previously listed for wearable sensor design are addressed (e.g., low cost, efficiency and user acceptance). In addition, the network should operate and coexist with other networks in similar frequency bands [6]. Here, a highly reconfigurable network architecture that opportunistically selects the best possible radiation characteristic for each link is considered. Reconfiguration is proposed in order to improve the reliability and enhance the battery lifetime, however, this functionality should not interfere with user convenience and cost. Therefore, the antennas proposed should support radiation pattern diversity along with other requirements.

Antenna design is one of the most important elements of the optimum wearable device, which should operate reliably for a long time without restricting user activity and causing any behavior modification. In order to increase the battery lifetime, the energy efficiency of the device should be improved. Considering the fact that the energy consumed during radio frequency (RF) transmission is a high percentage of the overall consumption, decreasing the number of retransmissions and improving the link budget by having higher antenna gain or pattern diversity can directly be translated into longer battery life.

A convenient form factor is also related to the antenna since it is one of the largest elements of the device alongside the battery. Flexible or small-sized rigid antennas are required so that the sensor can be incorporated seamlessly into clothing. When an antenna is located near lossy human tissues (i.e., worn by a person), its frequency response changes and radiation efficiency degrades. In order to avoid these, a body phantom should be included in the design process and the antenna should be electromagnetically isolated from the human body as much as possible with a ground plane. If the antenna is designed to be immune to these near-field effects of the body, the overall system efficiency is going to be maintained. In addition to being efficient and immune to detuning, the antenna can be reconfigurable in order to further improve system performance. The optimum radiation pattern will change depending on the link to be formed. Directional antennas were proven to perform the best for off-body links [7], whereas a radiation pattern with a null in the vertical plane according to the human body surface is best for on-body links [8]. Vertical polarization is better in launching surface waves [9]. In-body links are trickier since the propagation medium is extremely lossy. Therefore, as well as pointing the radiation toward the implant, one should minimize near-field losses either by increasing the separation between the antenna and the human body or by utilizing a bolus layer [10, 11].

The wearable reconfigurable antenna design challenge has been taken on by several researchers [12]. The proposed solutions can be grouped into two categories:

a. Flexible and comparatively larger antennas that can be printed on clothing.
b. Miniaturized rigid antennas that can be incorporated into clothing.

To the author's best knowledge, antennas that can achieve reconfigurability on flexible substrates are limited to five proposals [12–17]. A felt antenna operating at 2.45 GHz that can switch between four different radiation patterns has been proposed in [12]. The antenna has four different radiators each connected to its feed through a pin diode. As one pin diode is activated, the radiation of its corresponding radiator becomes dominant in the resultant radiation pattern. The patterns created are directive

patterns targeting $\Phi = 0°$, 90°, 180°, and 270°. One can argue that all these patterns are more suitable for **off-body links**. The size of the antenna is 88 mm × 88 mm × 2 mm. [13] described another 2.45 GHz felt antenna with an overall size of 100 mm × 100 mm × 3 mm. It switches between a monopolar and a directive radiation pattern. This is a critical property as it has the potential to cover both **on-body and off-body links**. In this chapter, however, the pin diodes were not realized. Hence, the efficiency figures of 38% and 45% for each mode are calculated excluding the switching stage. In [14], an antenna designed to operate at 6 GHz has been proposed. Due to the high operating frequency, its dimensions are 30 mm × 60 mm × 1.5 mm. It was printed on a mixed fabric made of polyester (66.2%) and cotton (33.8%). The antenna switches between three directive radiation patterns, two of them creating only a tilt of 30° in θ. All the patterns created are more suitable for **off-body links**. The prototype excludes the switching stage. In [15] an ultra-wideband (UWB) wearable antenna is prototyped using different techniques, such as conductive thread embroidery or thin laser-cut sheet of copper on cotton or denim substrate. Its size is relatively small: 42 mm × 80 mm × 1 mm. It achieves three different radiation patterns that steer on the H plane. The antenna does not have a strong directive mode, which is suitable for **on-body links**. Finally, [16, 17] described a flexible antenna operating at MedRadio band (401–406 MHz). This is an electrically small antenna with low gain values. It can switch between two radiation modes, however, the change in the maximum radiation direction is only 30°. All of these fabric antennas suffer from low efficiency values; however, they cover quite a wide range of prototyping techniques some of which overcome the problem of repeatability and durability [15]. Remember that the connection between the flexible and rigid structures remained a question mark. For example, the switching has been realized only in [12] where no repeatability analysis was performed.

On the other hand, the rigid reconfigurable wearable antennas being realized use more established manufacturing techniques that are more repeatable. They are expected to have greater efficiencies with smaller conductor losses associated with the radiator. However, for the rigid substrates, antenna sizes in the order of 100 mm are out of the question. Hence, the reconfigurable rigid wearable antennas in the literature are not more common than their flexible counterparts.

In [18], a dual port antenna with dimensions of 68 mm × 68 mm × 6.35 mm has been proposed. One of the ports excites a monopolar radiation pattern while the other one excites a directional one which can support both **on-body and off-body** links. The correlation between the ports is insignificantly small at the operating frequency of 2.45 GHz providing excellent diversity values. The efficiency of the antenna is greater than 92% for both modes, which is rare for wearable antennas. The antenna has two ports and the switching is excluded from the work. Another fine example of a rigid on-body antenna supporting both **on-body and off-body** links was presented in [19]. It is a circular antenna with a diameter of 48 mm and a thickness of 3.2 mm. Its performance is remarkable. Another rigid on-body antenna suitable for use in the 2.4 GHz industrial, scientific and medical (ISM) band has been proposed in [20]. The proposal is 120 mm × 155 mm × >6 mm. Although the size is too large to be used in practice, the antenna is unique in comprising a high impedance surface as its ground plane. It has two modes both of which have the same θ (43°) and opposite Φ (0°, 180°). Considering the tilt angle, both modes are suitable for **off-body** links.

When it comes to in-body links, reconfiguration efforts focus on reconfiguring the antenna's pattern and operating frequency together. UWB, Medical Implant Communication System (MICS), 2.4 or 5.8 ISM band have previously been used for in-body links; hence, reconfigurable antennas in the literature combine these frequencies with 2.4 or 5.8 GHz ISM bands intended for either on-body or off-body links. [21] described a dual band antenna which has an **in-body** mode at the MICS band and a directive off-body mode operating at 2.45 GHz. The size of the antenna, 40 mm × 40 mm × 3.2 mm, is comparable to other 2.4 GHz ISM band counterparts. [22, 23] proposed to use the 2.45 GHz ISM band for in-body communications. [22] described an antenna creating an off-body mode at the upper UWB band. It has a circular shape with a diameter of 35 mm and a very low profile of 0.76 mm thickness. On the other hand, [23] utilized the 5.8 GHz ISM band for on-body communications. The in-body mode has circular polarization while the on-body mode has a monopolar radiation pattern. The overall dimensions of the antenna are 29 mm × 31.3 mm × 5.8 mm. Despite the common assumption of operating the in-body mode at lower frequency bands, [24] proposed an antenna with an on-body mode at 2.45 GHz and an in-body mode at 5.8 GHz. The on-body mode has a monopolar radiation pattern and the in-body mode directs its energy toward the human body. The thick profile (15.5 mm × 10.5 mm × 28 mm) can be counted as a drawback, especially for a wearable antenna. Note that none of the proposed reconfigurable wearable antennas comprising an in-body mode is flexible.

The author has proposed several rigid and flexible pattern reconfigurable antennas that are comparable to the literature. Antennas that provide diversity for off-body links [25, 26], for off-body and on-body links [27–30], and off-body and in-body modes [31] are intended for various applications, including smart glasses and wristwatches charged with far-field wireless power transfer. The details of these antennas are going to be provided in Sections 14.2.1, 14.2.2, and 14.2.3.

14.2 EXAMPLE ANTENNAS

Examples provided here were simulated on Ansys human body phantom, male, 4 mm accuracy consideration, in all cases [11], as seen in Figure 14.1. The Specific Absorption Rate (SAR) of all the antennas discussed here are kept well under the 1.6 W/kg limitation averaged over 1 g of tissue [32].

The examples that will be provided here have been designed to create a complete BAN in which the sensors form wireless connections; thus, making use of the reconfigurability of antennas to maximize system performance. The envisaged BAN can be seen in Figure 14.2.

14.3 PROVIDING DIVERSITY FOR OFF-BODY LINKS

14.3.1 The Design of a Pattern Reconfigurable Antenna Suitable for Smart Glasses

A novel pattern reconfigurable wearable antenna suitable for a smart glasses application is designed to operate at the 2.4 GHz ISM band [26]. The antenna consists

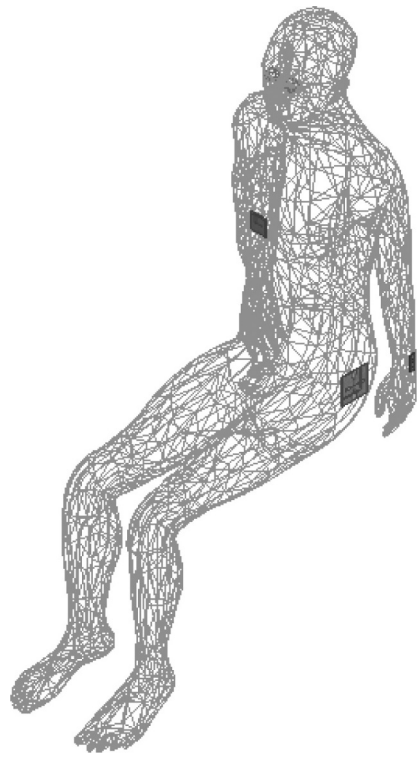

FIGURE 14.1 Wearables simulated on Ansys human body phantom: sitting position, male, 4 mm accuracy.

of two slots that are placed perpendicular to each other and fed with a coplanar waveguide transmission line placed at the corner as seen in Figure 14.3(a–b). The switches that are located directly on the slots are manipulated to activate different polarizations; hence, they provide polarization diversity. The gain patterns of each mode were simulated in a vacuum and their corresponding frequency responses can be seen in Figure 14.3(c–e). The antenna is prototyped on the glass as seen in Figure 14.3(b) and the simulations are validated through measurements. The antenna has been shown to provide two distinct patterns with a correlation coefficient of less than 0.1. Note that a pattern reconfigurable glass antenna has not been proposed before.

14.3.2 A Wrist Wearable Dual Port Dual Band Stacked Patch Antenna for Wireless Information and Power Transmission

A novel antenna with orthogonally polarized dual ports, one of which is dual band, is proposed [25]. It has a stacked patch configuration creating a dual band dual port operation unlike the heretofore aim of achieving a wideband operation.

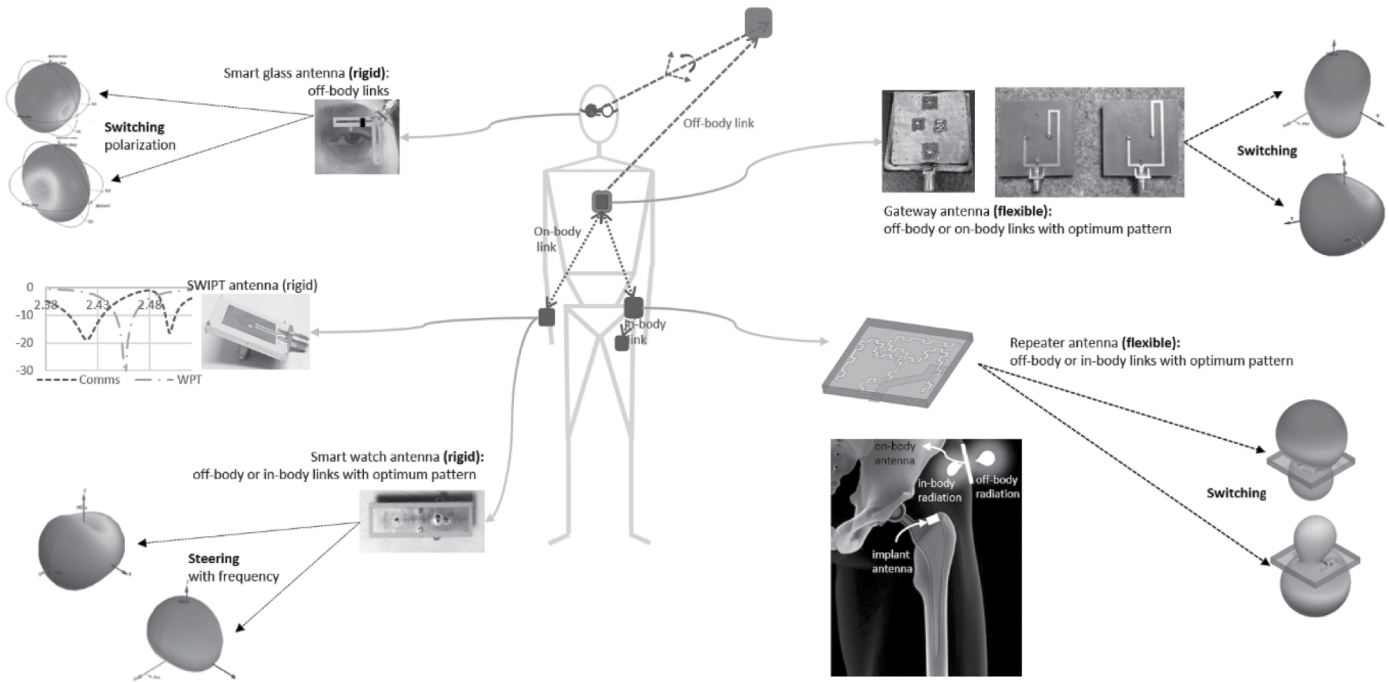

FIGURE 14.2 Reconfigurable wearable antennas previously proposed by the author presented at the system level.

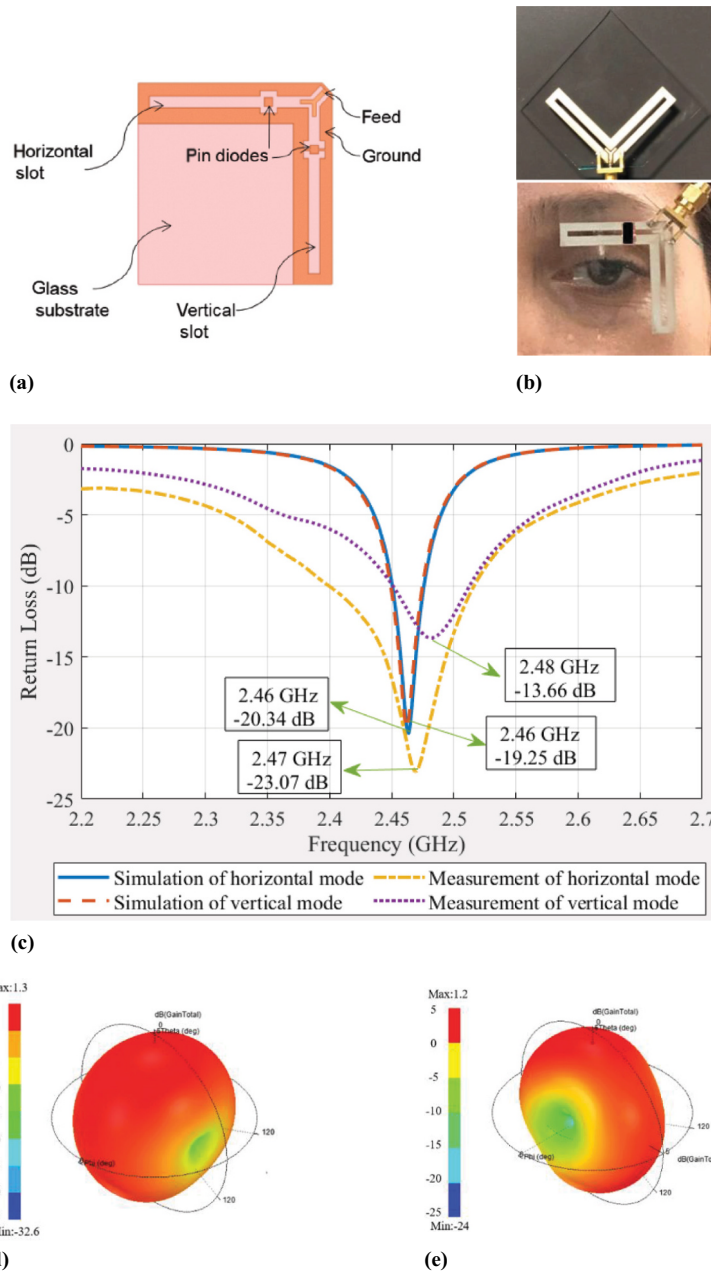

FIGURE 14.3 Pattern reconfigurable glass antenna suitable for smart glass applications providing polarization diversity of off-body links. (a) Antenna model including the pin diode pads, (b) antenna prototype without the pin diodes, (c) the simulated and measured frequency response of the antenna for each off-body mode, (d) simulated gain pattern of the horizontal slot while the vertical slot is shorted at 2.45 GHz, and (e) simulated gain pattern of the vertical antenna while the horizontal slot is shorted at 2.45 GHz.

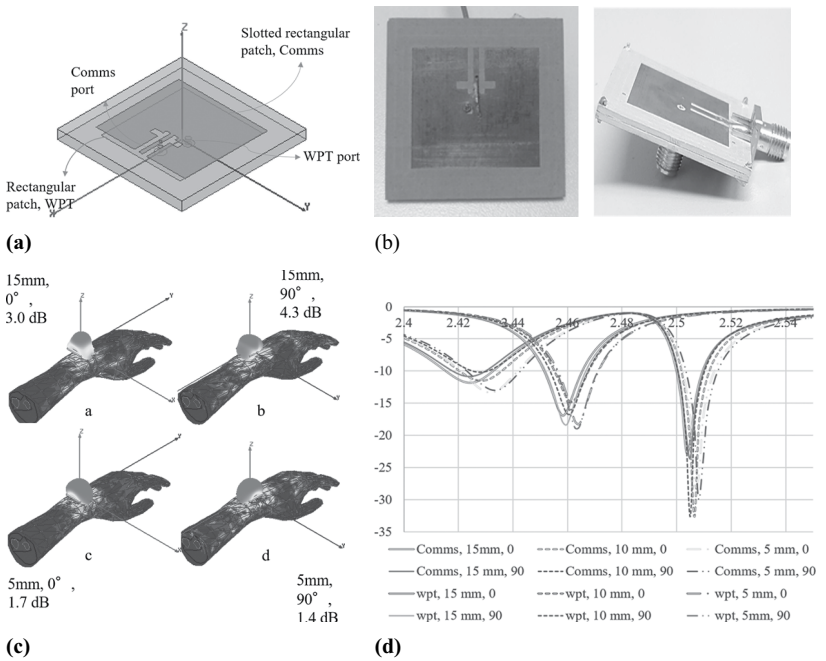

FIGURE 14.4 A wrist wearable dual port dual band stacked patch antenna for wireless information and power transmission. (a) A rectangular patch stacked with a dual band U slot loaded patch, (b) prototyped antenna, (c) the gain patterns and the magnitude of the current density, on the skin surface for each antenna–body separation of the communications port, and (d) the frequency response of the antenna on an arm phantom, the antenna–body separation is changed from 5 to 15 mm and the antenna is rotated 90° around z.

Here an upper U slotted rectangular patch is stacked with a lower rectangular patch as seen in Figure 14.4(a–b). The data port excites the upper patch covering Bluetooth Low Energy (BLE) advertisement channels while having a notch at around 22nd Channel (2.45 GHz) generated by the U slot etched at the edge of the upper patch. The wireless power transmission (WPT) port resonating at 2.45 GHz excites the lower patch. Isolation of more than 35 dB is achieved at the ports of the antenna before any further filtering, eliminating the need for an additional discrete diplexer.

The performance of the antenna is analyzed on the left arm of the Ansys computational human phantom as seen in Figure 14.4(c). The separation between the antenna and the wrist is changed from 5 to 15 mm in 5 mm steps while the arm is rotated for 90° for each separation in order to interrogate the effects of polarization. The frequency response of the antenna for these cases are plotted in Figure 14.4(d). It is observed that the detuning is more severe for WPT if there is no rotation, and more severe for the communications port if there is a 90° rotation. We can conclude that, for a wrist wearable antenna, if the polarization of the off-body mode is aligned with the arm, the detuning is stronger.

14.4 SWITCHING BETWEEN ON-BODY AND OFF-BODY LINKS

14.4.1 Pattern Diversity Antenna for On-Body and Off-Body Wireless BAN (WBAN) Links

A novel pattern reconfigurable flexible antenna is presented that can switch between two different radiation patterns. For the on-body and the off-body links, the TM_{00} and the TM_{01} modes (transverse magnetic modes) of a rectangular patch antenna are excited, respectively. The TM_{00} mode generates a quasi-omnidirectional pattern with a simulated directivity of 2 dB in the horizontal plane while the TM_{01} mode generates a directional pattern with a maximum directivity value of 4.5 dB. Both modes are matched at the 2.45 GHz ISM band. Finally, using numerical and physical phantoms and male subjects, the antenna has been shown to perform well near human bodies: insignificant detuning was observed and the degradation in the radiation efficiency was measured to be 17% in the worst-case scenario of locating the antenna on the body with 0 mm separation. Note that the size of the antenna is no bigger than a conventional half-wavelength patch antenna.

The TM_{00} mode of a shorted rectangular patch antenna creates an omnidirectional radiation pattern. Although the TM_{00} mode of a shorted rectangular patch has not been investigated extensively, it is analogous to the widely studied TM_{01} mode of shorted ring patch antennas. The TM_m mode describes the generation of the omnidirectional mode in non-circular patches. The application of it to BANs was discussed in [33] and it was compared with a rectangular patch and a monopole near the body surface. The shorted patch was shown to be superior for on-body links. Here, an antenna capable of generating this omnidirectional mode and a directional mode is designed.

As seen in Figure 14.5(a–b), it comprises a square patch and a full square ground plane underneath. The radiating patch is printed with a copper plate. The patch and the ground plane are separated with 4.8-mm-thick polyethylene foam by Emerson & Cuming. The ground plane is shorted to the patch at symmetrical shorting pins. The shorting pin positions and their radii are optimized through simulations. Beneath the ground plane, a feeding network is etched on a 1.6-mm-thick flame retardant-4 (FR-4) substrate with 35-μm-thick copper. The ground plane of the patch is used as the ground plane of the microstrip line feeding network, as well. The network excites the patch at two symmetrical points while these feeding points are isolated from the ground plane with two circular slots. The feed line comprises a T junction and its branches of unequal length are connected to the aforementioned symmetrical feed points. Being unequal, the lengths of the branches cause a phase difference, which can be changed by altering the length of one branch by utilizing a switching mechanism as seen in Figure 14.5(a). Two prototypes with altered branches were manufactured to test both modes. In addition to that, the antenna is prototyped on a flexible substrate, replacing both the polyethylene foam and FR-4 with felt. Copper is replaced with silver fabric and silver ink in an attempt to compare the two as seen in Figure 14.5(c–d).

Figure 14.5(e–f) shows the E field distribution in vector form created by each mode: TM_{00} and TM_{01}. Feeding the excitation points with a 0° phase difference will

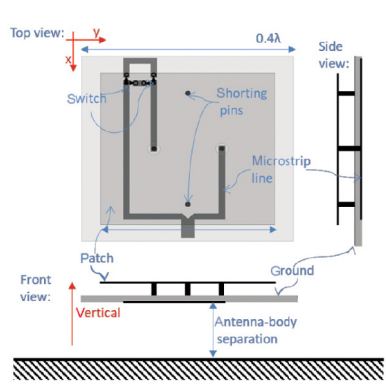

(a)

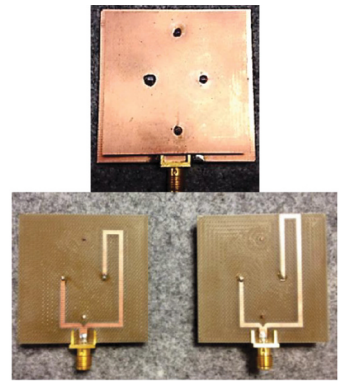

(b)

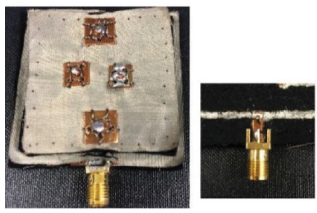

(c)

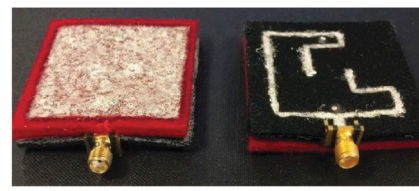

(d)

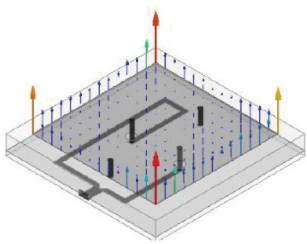

(e)

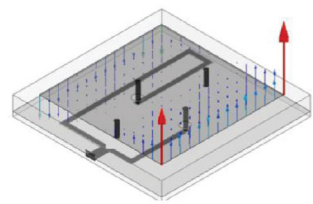

(f)

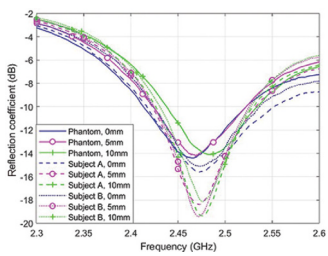

(g)

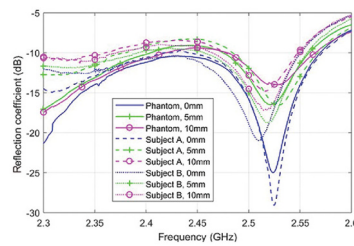

(h)

FIGURE 14.5 Pattern diversity antenna for on-body and off-body wireless body area network links [28]. (a) The proposed dual mode antenna which comprises a switching mechanism. (b) The prototyped on-body and off-body antennas, rigid version. (c) The prototyped on-body and off-body antennas, flexible version with silver fabric on felt. (d) The prototyped on-body and off-body antennas, flexible version with silver paint on felt. (e) Vector E field distributions of TM_{00}, on-body mode. (f) Vector E field distributions of TM_{01}, off-body mode. (g) |S11| (dB) vs. frequency (GHz) of the on-body mode. (h) |S11| (dB) vs. frequency (GHz) of the off-body mode.

(*Continued*)

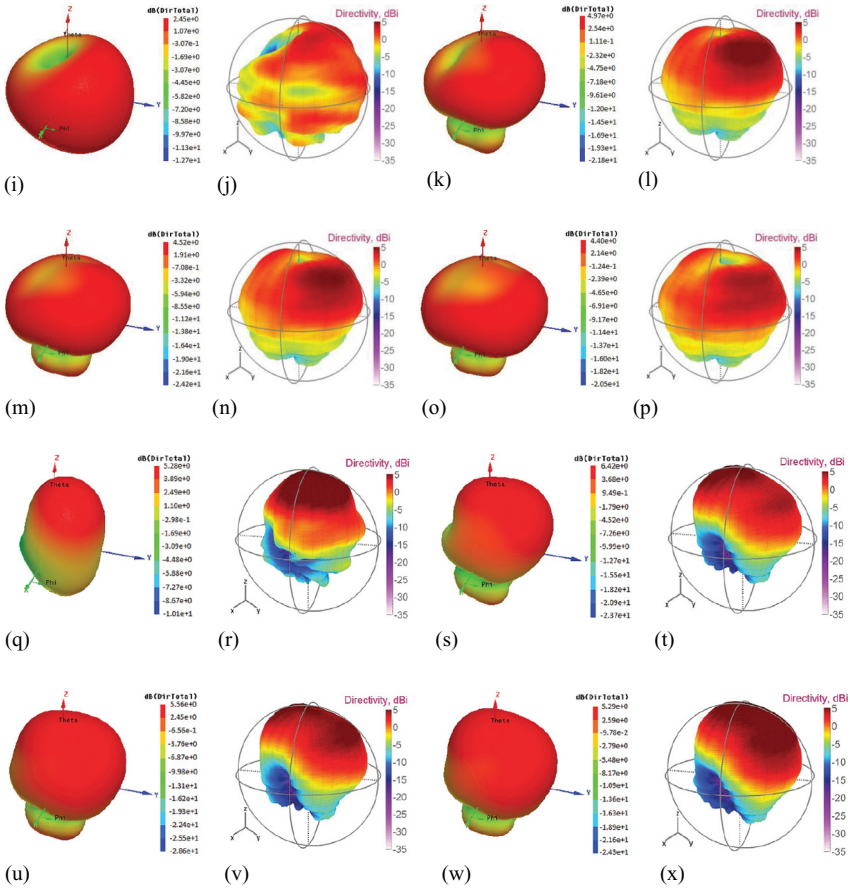

FIGURE 14.5 (CONTINUED) (i) On-body antenna in vacuum, simulation. (j) On-body antenna on RAM, meas, max. dir. of 4 dBi. (k) On-body antenna on the phantom with 0 mm antenna–body separation, simulation. (l) On-body antenna on the phantom with 0 mm antenna–body separation, Meas, max. dir. of 5.5 dBi. (m) On-body antenna on the phantom with 5 mm antenna–body separation, simulation. (n) On-body antenna on the phantom with 5 mm antenna–body separation, meas, max. dir. of 5 dBi. (o) On-body antenna on the phantom with 10 mm antenna–body separation, simulation. (p) On-body antenna on the phantom with 10 mm antenna–body separation, meas, max. dir. of 4 dBi. (q) Off-body antenna in vacuum, simulation. (r) Off-body antenna on RAM, meas, max. dir. of 8 dBi. (s) Off-body antenna on the phantom with 0 mm antenna–body separation, simulation. (t) Off-body antenna on the phantom with 0 mm antenna–body separation, meas, max. dir. of 7.6 dBi. (u) Off-body antenna on the phantom with 5 mm antenna–body separation, simulation. (v) Off-body antenna on the phantom with 5 mm antenna–body separation, meas, max. dir. of 7 dBi. (w) Off-body antenna on the phantom with 10 mm antenna–body separation, simulation. (x) Off-body antenna on the phantom with 10 mm antenna–body separation, meas, max. dir. of 6.5 dBi. Meas, max. dir. is measured maximum directivity.

activate TM_{00}. Practically, the phase difference can be greater than 0° for matching purposes as long as it is less than 90°. Once it is greater than 90°, the uniformity of the radiation pattern along φ will be severely distorted. On the other hand, having E field vectors in opposite directions at the excitation points will activate the TM_{01} mode. Hence, the phase difference should be 180°. Similarly, this value can be decreased for matching purposes as long as it is more than 90°, which will generate a more directional radiation pattern suitable for off-body operation. Here the length of the longer branch is decreased by λ/4 to switch between these two modes. Note that the length of the shorter branch is 28 mm and the longer branch is changed from 73 to 85 mm.

Figure 14.5(g–h) demonstrates the antenna's measured frequency response for different scenarios to the variation in the antenna–body separations. As previously predicted by the simulations, the on-body antenna's return loss is not as great as the off-body antenna's; however, both antennas are fairly stable against the changes in their near-field. The center frequency of the off-body antenna remains at 2.52 GHz for the phantom and Subject A, while it shifts to 2.51 GHz for Subject B. Note that Subject B has less fat in his body composition. For the on-body antenna, the center frequency remains at 2.47 most of the time, which shows that the on-body antenna is more immune to changes in body composition. In terms of the frequency response, the antenna satisfies the requirements of a BAN antenna and can be used near lossy environments. The return losses of both antennas for all scenarios are above 10 dB at 2.5 GHz. Therefore, 2.5 GHz is chosen as the frequency of measurement for the prototyped off-body and on-body antennas during the radiation pattern measurements.

Figure 14.5(l–x) show the gain patterns of the on-body and off-body antennas in vacuum, on RAM, and on the previously described single-layer flat phantom mimicking the chest of an individual. In Figure 14.5(l) the on-body antenna generates an omnidirectional radiation pattern in its horizontal plane at 2.5 GHz. The complimentary measurement is shown in Figure 14.5(j). Although the antenna generates a null at $\theta = 0°$ as predicted, the pattern is distorted. This is due to the fact that the antenna is measured on a block of RAM backed with a metal rotating post carrying the antenna. Therefore, the antenna does not act in a way identical to the way it acts in vacuum. When the on-body antenna is positioned on the phantom, the agreement between the simulations and the measurements gets much better. Comparing Figure 14.5(l) and (k), it can be observed that once the antenna is positioned on the body phantom, its radiation is shifted in the vertical direction and the energy will be emitted mostly in the positive half-space. This is favorable considering the SAR. Finally, Figure 14.5(k-p) show that the null at $\theta = 0°$ is maintained in all cases. In vacuum, the off-body antenna generates a directional pattern at 2.5 GHz and the measured half-power beam width is approximately 100°, see Figure 14.5(q) and (r). Comparing these figures, the agreement between the simulation in vacuum and the measurement on RAM is better compared to the on-body antenna case since the off-body antenna's radiation in the lower half-space is minimal. When the off-body antenna is located on the phantom, the pattern goes through slight changes as predicted by the simulations. However, its directional nature is maintained, making it suitable for off-body communications. In all measured results, the effect of the feed connector is visible, which

is positioned along the negative x-axis of the radiation pattern. This distortion leads to a slight increase in the cross-polarization levels of the off-body antenna. When the off-body antenna and the on-body antenna are simulated and measured on the phantom with different separations from 0 to 10 mm with 5-mm increments, the radiation patterns remain directional and omnidirectional, respectively.

Both antennas show little backward radiation, which restricts the absorption by the phantom. This is because the proposed antennas incorporate a full ground plane below their main radiator.

Note that this antenna currently is the smallest flexible antenna providing diversity for on-body and off-body links to the author's knowledge.

14.4.2 A Radiation Pattern Diversity Antenna Operating at the 2.4 GHz ISM Band

A novel rigid antenna meant to be worn on the wrist, operating in the 2.4 GHz ISM band, whose radiation pattern can be steered as the frequency of operation changes has been proposed [29]. This is achieved by merging the different radiation modes of the antenna together within a single operating band as seen in Figure 14.6(a–b), in contrast to the conventional procedure of covering the whole band with a single radiation mode. Using this method, a single antenna can provide radiation pattern diversity across the operating band without an external switching mechanism. The proposed antenna is a probe-fed patch shorted at four symmetrical points as seen in Figure 14.6(c–d). It is analyzed in terms of its on-body and off-body propagation performance as well as its sensitivity to antenna–body spacing. The antenna is shown to perform well up to 5 mm spacing. It has been proved that the antenna provides 9 dB advantage on average for the on-body link compared to the case where its off-body radiation mode is used to connect to the on-body sensor and vice versa. Moreover, the antenna is benchmarked against a monopole and a patch antenna in a residential setting. The performance of the antenna and subsequently the benefits of the pattern-switching technique are successfully quantified. The holistic method includes both antenna measurements and channel simulation with ray tracing. The results are verified against real-world measurements [30].

By changing the frequency within the ISM band, the maximum radiation direction is changed. If BLE standards are used, the first ten channels (Channel 37, Channels 0–8) can be used for the azimuth mode and the remaining 30 channels (Channels 9–39) can be used for the elevation mode. If ZigBee is preferred, Channels 11–14 can be used for the azimuth mode while Channels 15–26 will be more suitable for the elevation mode. Note that the Zigbee Channels 1–10 are located in the 915 MHz ISM band. The number of channels can be adjusted according to the needs of the system by changing the operating frequency of each mode. Looking into the interference rejection aspect of the application, approximately 10 dB difference is observed between the modes at $\theta = 0°$. If there is an interferer arriving at the antenna from the $\pm z$ direction, it is going to be attenuated by the antenna. Likewise, approximately 5 and 10 dB difference are observed between the modes at $\theta = 90°$ and $\theta = -90°$, respectively. Note that these numbers are subject to the specific channels chosen.

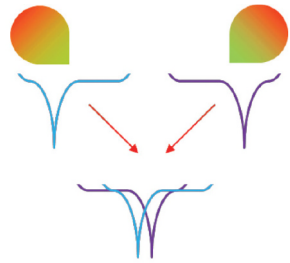

(a)

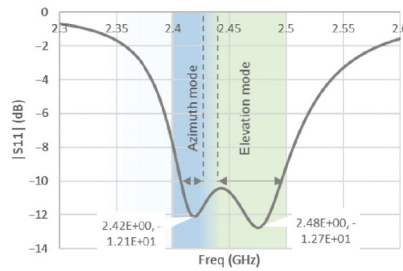

(b)

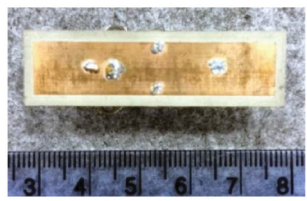

(c)

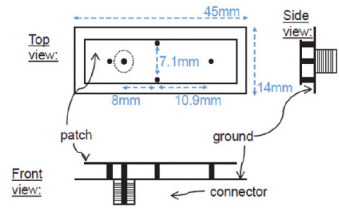

(d)

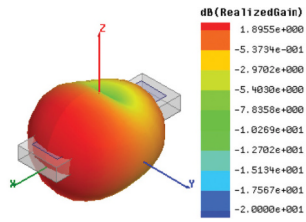

TM_m mode, θ= 72⁰ The azimuth mode.

(e)

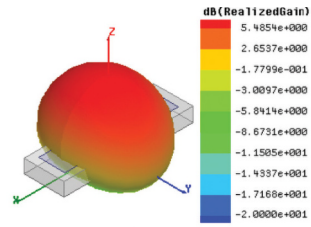

TM_{01} mode, θ = 8⁰ The elevation mode

(f)

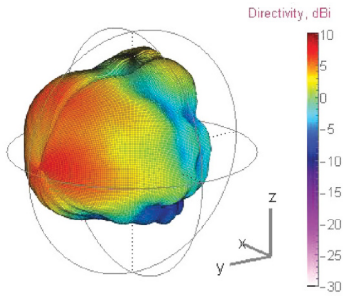

(g)

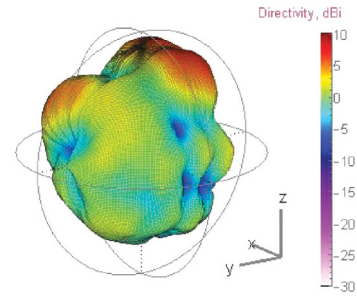

(h)

FIGURE 14.6 A radiation pattern diversity antenna operating at the 2.4 GHz industrial, scientific and medical band [29, 30]. (a) Merging the different radiation modes of the antenna together within a single operating band. (b) TM_m mode is excited along with the dominant TM_{01} mode in 2.4 GHz industrial, scientific and medical band. (c) Shorted patch antenna prototyped on Rogers RT/Duroid 6006. (d) Antenna model. (e) Simulated gain pattern of the on-body mode: TM_m. (f) Simulated gain pattern of the off-body mode: TM_{01}. (g) Measured gain pattern of the on-body mode, TM_m. (h) Measured gain pattern of the off-body mode, TM_{01}.

(*Continued*)

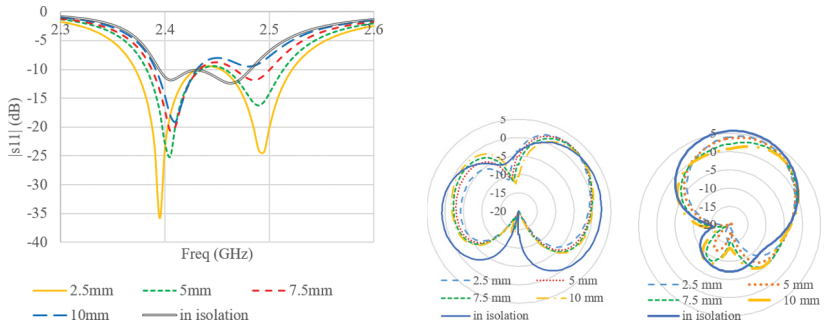

FIGURE 14.6 (CONTINUED) (i) Effect of antenna–body separation on the return loss. (j) Effect of antenna–body separation on the gain (on-body at 2.4 GHz, off-body at 2.48 GHz).

For the first selected frequency of 2.4 GHz, 2.6 dB maximum gain is observed. The maximum gain direction is $\theta = 72°$, $\Phi = 0°$ with minimal radiation in the vertical direction with respect to the body surface as seen in Figure 14.6(e–h). This stops energy from being wasted in the body or transmitted away from the body. It directs the energy toward the other on-body antennas along the body. Moreover, it has vertical polarization which is favored over horizontal polarization for on-body communications due to the excitation of the surface waves. On the other hand, at the second selected frequency 2.48 GHz, the radiation pattern is optimized for connecting to an off-body gateway with 5.8 dB maximum gain at $\theta = 8°$, $\Phi = 0°$.

The effect of antenna–body spacing has also been analyzed. The antenna–body separation is changed with 2.5 mm steps from 2.5 to 10 mm and the frequency characteristics demonstrating the two different modes and their frequency coverage for these antenna–body separations can be seen in Figure 14.6(i). As the antenna–body separation is decreased, the modes are shifted away from each other. The efficiency of the antenna degrades as the separation between the ground plane and the phantom decreases as seen in Figure 14.6(j). This is expected due to the lossy nature of the tissues in the phantom. However, in all cases, the efficiency is greater than 50%. We can see that the degradation in efficiency once the antenna is located on the phantom is greater for the off-body mode. This is due to the off-body mode having a higher electric field and lower magnetic field in the near-field of the antenna. Note that magnetic near fields are less susceptible to dissipation on the human body since human tissues have no magnetic losses ($\mu_r'' = 0$).

This antenna provides a unique middle ground between size and reconfigurability. The approach can be applied to other radiators.

14.5 SWITCHING BETWEEN IN-BODY AND OFF-BODY LINKS

The wireless link between an implant and an off-body gateway may be difficult to secure due to the fact that electromagnetic waves quickly attenuate as they propagate through human tissues. Depending on the depth of the implant within the body, the signal strength may be quite weak by the time the waves reach the skin. In order to

address this problem, a digitally assisted repeater antenna has been designed [31] to be located outside the patient's body, which can detect the signals radiated by the implant and relay those signals to the off-body gateway. The antenna is based on U.S. Patent US10149636B2. The radiation pattern of the antenna is switched between two modes depending on the link it is forming: in-body link or off-body link. With an overall size of 30 × 30 × 3.15 mm, the antenna operates in the 2.4 GHz ISM band. The repeater is aimed to be used to secure wireless communications with a smart deep implant. Therefore, for a typical depth of such an implant, which is 4 cm, the repeater has been shown to enable a decrease of more than 40 dB in the transmit power level while the distance between the implant and the off-body gateway is kept constant.

Two slots are carved into the opposite faces of a single rectangular shallow cavity and both slots are fed with the same stripline which meanders in between the slots as seen in Figure 14.7(a). The slots are activated in an alternating way by means of two switches located in the center of each slot. When a switch is turned on, the slot on the opposite side is activated. This is a novel and a simple way of achieving radiation pattern diversity in a cavity-backed slot antenna. Having a shorted slot on the opposite wall of the cavity does not affect the activated slot since the shorted slot operates at a higher frequency and its polarization is orthogonal to the active slot.

The frequency response of each slot while the other one is shorted with a switch is plotted in Figure 14.7(b). The generated radiation patterns are plotted in 3D in Figure 14.7(c–d). Note that these radiation patterns are generated while the antenna is located in vacuum. Surely, the response will change once the antenna is located near lossy body tissue. Further analysis has been performed in order to demonstrate the performance of the antenna as a repeater. In a realistic scenario, the repeater is expected to be located near the human body to collect data from the implant. Locating the antenna near the lossy tissues deteriorates the performance of the antenna, especially during the in-body mode of operation. Therefore, the antenna's reflection coefficient is monitored while the separation between the skin and the antenna is changed. As seen in Figure 14.7(b), 40 mm has been found to be an acceptable separation with minimal detuning. Figure 14.7(e–f) shows the E field distribution in the vertical plane within a transmission scenario where a 4 cm deep implantable antenna operating at 2.4 GHz is excited and the repeater is located 4 cm away from the skin. These demonstrate how the energy is focused toward the desired direction.

The antenna is meant for prototyping on a felt substrate, and expected simulated efficiencies are 90% for the off-body mode and 72% for the in-body mode with 4 cm separation. The antenna can be located closer to the human body by replacing the gap with a bolus layer which is still work under progress for this particular project.

This antenna currently is the only flexible repeater antenna that can accommodate for the in-body and off-body communications to be formed at the same frequency band.

14.6 CONCLUSION

A challenging aspect of antenna design in wearable devices is the dynamic nature of the human body leading to dynamic propagation channels. Antenna requirements are

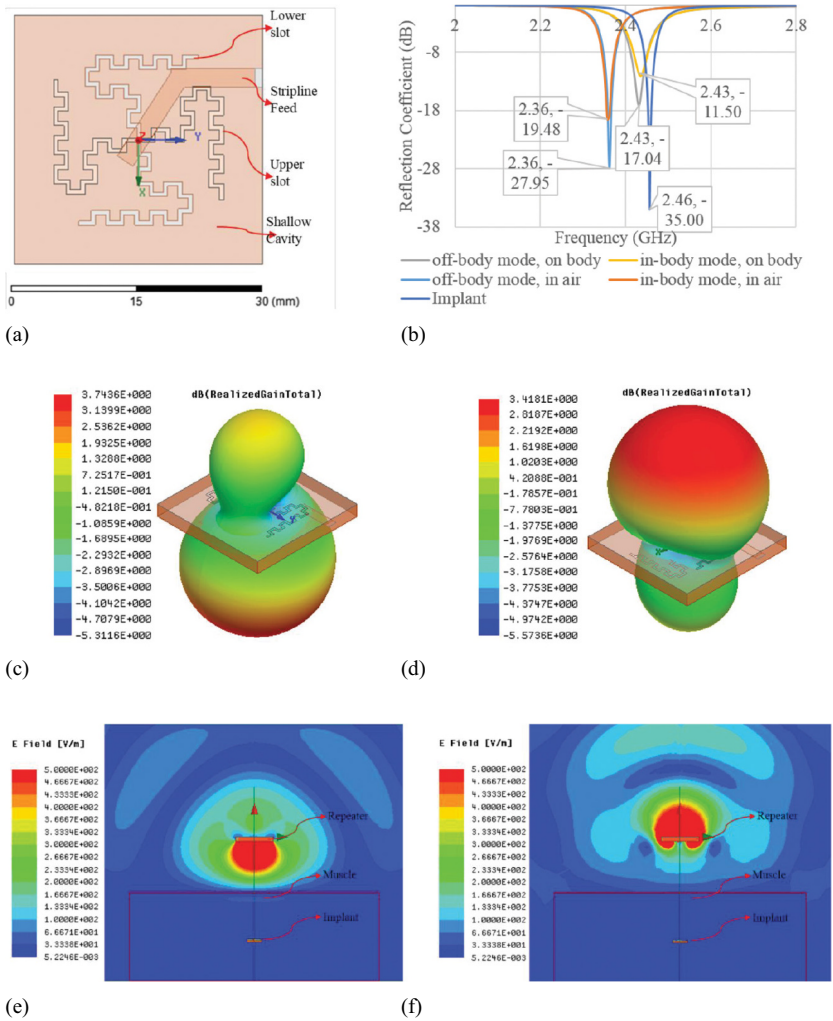

FIGURE 14.7 A digitally assisted repeater antenna for implant communications. (a) Antenna diagram, slots miniaturized according to second order Koch-fractal configuration. (b) The reflection coefficient of the in-body and off-body mode when the antenna is located in air and on human body with 4 cm separation. (c) The simulated gain pattern of the in-body mode when the antenna is located in vacuum. (d) The simulated gain pattern of the off-body mode when the antenna is located in vacuum. (e) E field distribution for in-body mode. (f) E field distribution for off-body mode.

different and sometimes contradictory for the connections established by different wearables placed at various points in the human body. In order to tackle this challenge, re-shaping the radiation pattern according to the direction of arrival of the wanted signal is a logical step forward. However, with small space available on the wearable devices and the limited energy supply, realizing these objectives are difficult

since they require complex hardware and intensive calculation. Here, an overview of reconfigurable wearable antennas proposed in the literature is given. In addition, five different reconfigurable antennas previously proposed by the author are provided as examples. The examples cover antennas providing diversity for off-body links, switching between off-body and on-body links and between off-body and in-body links.

REFERENCES

[1] CodeBlue: Wireless Sensors for Medical Care, https://dash.harvard.edu/bitstream/handle/1/3191012/1242078272-bsn.pdf?sequence=2, accessed January 2020.
[2] The Human ++ Project, https://www.thehumanproject.org/, accessed January 2020.
[3] SPHERE – A Sensor Platform for HEalthcare in a Residential Environment, https://www.irc-sphere.ac.uk/, accessed January 2020.
[4] C. Van Hoof, "Wearable Wireless Sensor Technologies for Truly Personalized Medicine and Wellness," in *Radio Wireless Symposium*, San Diego, CA, 2015.
[5] S. Dumanli, S. Gormus, and I. J. Craddock, "Energy Efficient Body Area Networking for mHealth Applications," in *Medical Information and Communication Technology (ISMICT), 2012 6th International Symposium on*, La Jolla, CA, pp. 1–4, March 25–29, 2012.
[6] M. R. Yuce, "Wearable and Implantable Wireless Bod Area Networks," *Recent Patents on Electrical Engineering*, 2, 115–124, 2009.
[7] E. Mellios, A. Goulianos, S. Dumanli, G. S. Hilton, R. J. Piechocki, and I. J. Craddock, "Off-Body Channel Measurements at 2.4 GHz and 868 MHz in an Indoor Environment," in *Proceedings of the 9th International Conference on Body Area Networks*, London, 2014, pp. 5–11.
[8] P. S. Hall, Y. Hao, Y. I. Nechayev, A. Alomainy, C. C. Constantinou, C. Parini, M. R. Kamarudin, T. Z. Salim, D. T. M. Hee, R. Dubrovka, A. S. Owadally, S. Wei, A. Serra, P. Nepa, M. Gallo, and M. Bozzetti, "Antennas and Propagation for On-Body Communication Systems," *IEEE Antennas and Propagation Magazine*, 49(3), 41–58, June 2007.
[9] T. Alves, B. Poussot, and J. M. Laheurte, "Analytical Propagation Modeling of BAN Channels Based on the Creeping-Wave Theory," *IEEE Transactions on Antennas and Propagation*, 59(4), 1269–1274, 2011
[10] F. Merli, B. Fuchs, J. R. Mosig, and A. K. Skriverviky, "The Effect of Insulating Layers on the Performance of Implanted Antennas," *IEEE Transactions on Antennas and Propagation*, 59(1), 21–31, January 2011.
[11] W. Xia, K. Saito, M. Takahashi, and K. Ito, "Performances of an Implanted Cavity Slot Antenna Embedded in the Human Arm," *IEEE Transactions on Antennas and Propagation*, 57(4), 894–899, April 2009.
[12] M. I. Jais, M. F. Jamlos, M. Jusoh, T. Sabapathy, and M. R. Kamarudin, "2.45 GHz Beam-Steering Textile Antenna for WBAN Application," in *2013 IEEE Antennas and Propagation Society International Symposium (APSURSI)*, Orlando, FL, 2013, pp. 200–201.
[13] S. Yan and G. A. E. Vandenbosch, "Wearable Pattern Reconfigurable Patch Antenna," in *2016 IEEE International Symposium on Antennas and Propagation (APSURSI)*, Fajardo, 2016, pp. 1665–1666.
[14] S. Ha and C. W. Jung, "Reconfigurable Beam Steering Using a Microstrip Patch Antenna With a U-Slot for Wearable Fabric Applications," *IEEE Antennas and Wireless Propagation Letters*, 10, 1228–1231, 2011.
[15] A. da Conceição Andrade, I. P. Fonseca, S. F. Jilani, and A. Alomainy, "Reconfigurable Textile-Based Ultra-Wideband Antenna for Wearable Applications," *2016 10th European Conference on Antennas and Propagation (EuCAP)*, Davos, 2016, pp. 1–4.

[16] S. Kang and C. W. Jung, "Wearable Fabric Antenna on Upper Arm for MedRadio Band Applications with Reconfigurable Beam Capability," *Electronics Letters*, 51(17), 1314–1316, 2015.
[17] S. Kang and C. W. Jung, "Wearable fabric reconfigurable beam steering antenna for on/off-body communication system," in *2015 IEEE International Symposium on Antennas and Propagation & USNC/URSI National Radio Science Meeting*, Vancouver, BC, 2015, pp. 1211–1212.
[18] R. Masood, C. Person, and R. Sauleau, "A Dual-Mode, Dual-Port Pattern Diversity Antenna for 2.45-GHz WBAN," *IEEE Antennas and Wireless Propagation Letters*, 16, 1064–1067, 2017.
[19] X. Tong, C. Liu, X. Liu, H. Guo, and X. Yang, "Switchable ON-/OFF-Body Antenna for 2.45 GHz WBAN Applications," *IEEE Transactions on Antennas and Propagation*, 66(2), 967–971, February 2018.
[20] M. Li, S. Xiao, and B. Wang, "Pattern-Reconfigurable Antenna for On-Body Communication," *2013 IEEE MTT-S International Microwave Workshop Series on RF and Wireless Technologies for Biomedical and Healthcare Applications (IMWS-BIO)*, Singapore, 2013, pp. 1–3.
[21] K. Kwon, J. Tak, and J. Choi, "Design of a Dual-Band Antenna for Wearable Wireless Body Area Network Repeater Systems," in *2013 7th European Conference on Antennas and Propagation (EuCAP)*, Gothenburg, 2013, pp. 418–421.
[22] J. M. Felício, J. R. Costa and C. A. Fernandes, "Dual-Band Skin-Adhesive Repeater Antenna for Continuous Body Signals Monitoring," *IEEE Journal of Electromagnetics, RF and Microwaves in Medicine and Biology*, 2(1), 25–32, March 2018.
[23] K. Li, L. Xu, Z. Duan, Y. Tang, and Y. Bo, "Dual-Band and Dual-Polarized Repeater Antenna for Wearable Applications," in *2018 IEEE MTT-S International Wireless Symposium (IWS)*, Chengdu, 2018, pp. 1–3.
[24] J. Tak, K. Kwon, and J. Choi, "Design of a Dual Band Repeater Antenna for Medical Self-Monitoring Applications," in *2013 IEEE Antennas and Propagation Society International Symposium (APSURSI)*, Orlando, FL, 2013, pp. 2091–2092.
[25] S. Dumanli, "A Wrist Wearable Dual Port Dual Band Stacked Patch Antenna for Wireless Information and Power Transmission," in *2016 10th European Conference on Antennas and Propagation (EuCAP)*, Davos, 2016, pp. 1–5.
[26] E. Cil and S. Dumanli, "The Design of a Pattern Reconfigurable Antenna Suitable for Smart Glasses," in *2019 IEEE 30th International Symposium on Personal, Indoor and Mobile Radio Communications (PIMRC Workshops)*, Istanbul, Turkey, 2019, pp. 1–4.
[27] S. Dumanli, "On-Body Antenna with Reconfigurable Radiation Pattern," in *2014 IEEE MTT-S International Microwave Workshop Series on RF and Wireless Technologies for Biomedical and Healthcare Applications (IMWS-Bio2014)*, London, 2014, pp. 1–3.
[28] S. Dumanli, "Pattern Diversity Antenna for On-Body and Off-Body WBAN Links." *Turkish Journal of Electrical Engineering & Computer Sciences*, 26(5), 2395–2405, 2018.
[29] S. Dumanli, "A Radiation Pattern Diversity Antenna Operating at the 2.4 GHz ISM Band," in *2015 IEEE Radio and Wireless Symposium (RWS)*, San Diego, CA, 2015, pp. 102–104.
[30] S. Dumanli, L. Sayer, E. Mellios, X. Fafoutis, G. S. Hilton, and I. J. Craddock, "Off-Body Antenna Wireless Performance Evaluation in a Residential Environment," *IEEE Transactions on Antennas and Propagation*, 65(11), 6076–6084, November 2017.
[31] S. Dumanli, "A Digitally Assisted Repeater Antenna for Implant Communications," in *2017 11th European Conference on Antennas and Propagation (EUCAP)*, Paris, 2017, pp. 181–184.
[32] FCC's SAR Guidelines, *OET Bulletin* 65, [online] https://transition.fcc.gov/bureaus/oet/info/documents/bulletins/oet65/oet65.pdf, accessed on January 2019.
[33] G. A. Conway and W. G. Scanlon, "Antennas for Over-Body-Surface Communication at 2.45 GHz." *IEEE Transactions on Antennas & Propagation*, 57, 844–855, 2009.